JACS
JOURNAL OF THE AMERICAN CHEMICAL SOCIETY
pubs.acs.org/JACS
Communication

Targeted and Equally Distributed Delivery of mRNA to Organs with Pentaerythritol-Based One-Component Ionizable Amphiphilic Janus Dendrimers

Juncheng Lu, Elena N. Atochina-Vasserman, Devendra S. Maurya, Dipankar Sahoo, Nathan Ona, Erin K. Reagan, Houping Ni, Drew Weissman,* and Virgil Percec*

Cite This: J. Am. Chem. Soc. 2023, 145, 18760−18766
Read Online

ABSTRACT: Delivery of nucleic acids with viral and synthetic vectors has pioneered genetic nanomedicine. Four-component lipid nanoparticles (LNPs) consisting of ionizable lipids, phospholipids, cholesterol, and PEG-conjugated lipids, assembled by microfluidic or T-tube, are the benchmark synthetic vector for delivery of mRNA. One-component multifunctional sequence-defined ionizable amphiphilic Janus dendrimer (IAJD) delivery systems for mRNA were developed by us to complement LNPs. IAJDs consist of multifunctional hydrophilic low-generation dendrons or minidendrons conjugated to hydrophobic dendrons. They were inspired by amphiphilic Janus dendrimers and glycodendrimers. IAJDs coassemble with mRNA into predictable-size vesicles, named dendrimersome nanoparticles (DNPs), by simple injection in acetate buffer, rather than by the complex technology required by LNPs. Assembly of DNPs by simple injection together with sequence design in the hydrophilic and hydrophobic modules of IAJDs endowed rapid screening to access discovery. Molecular design principles for targeted delivery were elaborated when the branching points of IAJDs were constructed from symmetrically and nonsymmetrically substituted plant phenolic acids interconnected by pentaerythritol (PE). Here, we report the first library containing simplified IAJDs constructed in only three steps from symmetrically trialkylated PE in the hydrophobic domain and four different piperazine-based ionizable amines in the hydrophilic part. Rapid coassembly with mRNA and *in vivo* screening led to the discovery of the two most active IAJDs targeting the spleen, liver, and lymph nodes, one predominantly to the spleen and liver and six delivering equally to the spleen, liver, lung, and lymph nodes. These IAJDs represent the simplest synthetic vectors and the first viral or synthetic system delivering equally to multiple organs.

The extraordinary success with Covid-19 vaccines orchestrated viral and four-component lipid nanoparticles (LNPs) (Figure 1a) into leading vectors for nucleic acid delivery.[1] Both viral and synthetic vectors display advantages and disadvantages. Viral vectors are stable with high transfection efficacy (95%)[2a] and cell targeting,[2b] while LNPs are less stable[2c] and transfection efficient (1−2%).[2d] Drawbacks of viral vectors include immunogenicity,[2e] cytotoxicity,[2f] difficult assembly,[2g] inflammatory responses[2c] to repeated administration, and potential for insertional mutagenesis.[2d] Advantages of synthetic vectors include higher biosafety, lower toxicity, and immunogenicity,[2d] while drawbacks involve the need for microfluidic or T-tube technology[3a−d] for assembly and low temperature for long-term storage (−70 °C).[3e] Some disadvantages of LNPs[3f,g] are endowed by the unknown distribution of components.[3h,i] For example, it is believed that at neutral pH the segregation of *transiently charged* ionizable amines (IAs) (charged at acidic pH to complex mRNA and neutral at physiological pH to become nontoxic)[3f,5a] as an oil phase in the core of the LNPs (Figure 1a) is responsible for their 1−2% transfection efficacy.[3h,i]

The PEG-conjugated lipid originates the "PEG dilemma".[3j−m] *Permanently charged* cationic lipids and dendrimers pioneered DNA delivery[4] but are toxic and unsuitable for delivery of less stable mRNA requiring encapsulation to protect from enzymatic degradation. The permanently and transiently charged mechanisms were described.[3f,5a] During the Covid-19 pandemic we decided to eliminate LNPs' weaknesses by incorporating their four activities into a one-component system.[5a] Sequence-defined amphiphilic Janus dendrimers (JDs)[6] and Janus glycodendrimers (JGDs),[7] discovered in one of our laboratories, were known to self-assemble stable and monodisperse vesicles with predictable size known as dendrimersomes (DSs)[6] and glycodendrimersomes (GDSs)[7] by simple injection of the JD or JGD ethanol solution into water or buffer. Before the pandemic, the roles of sequence and concentration of the carbohydrates of the JGDs on the activity of their GDSs during agglutination to sugar-binding proteins were elucidated.[7] During the pandemic, replacement of the carbohydrates of JGDs with IAs accessed the first class of IAJDs.[5a] Twin−twin (TT, two hydrophobic dendrons connected to two hydrophilic dendrons both containing ionizable amines via a pentaerythritol (PE) linker), twin-mixed, (TM, two hydrophobic dendrons conjugated to one hydrophilic dendron containing IAs and one hydrophilic without IAs), single−single (SS, one hydrophobic dendron

Received: July 11, 2023
Published: August 22, 2023

https://doi.org/10.1021/jacs.3c07337
J. Am. Chem. Soc. 2023, 145, 18760−18766

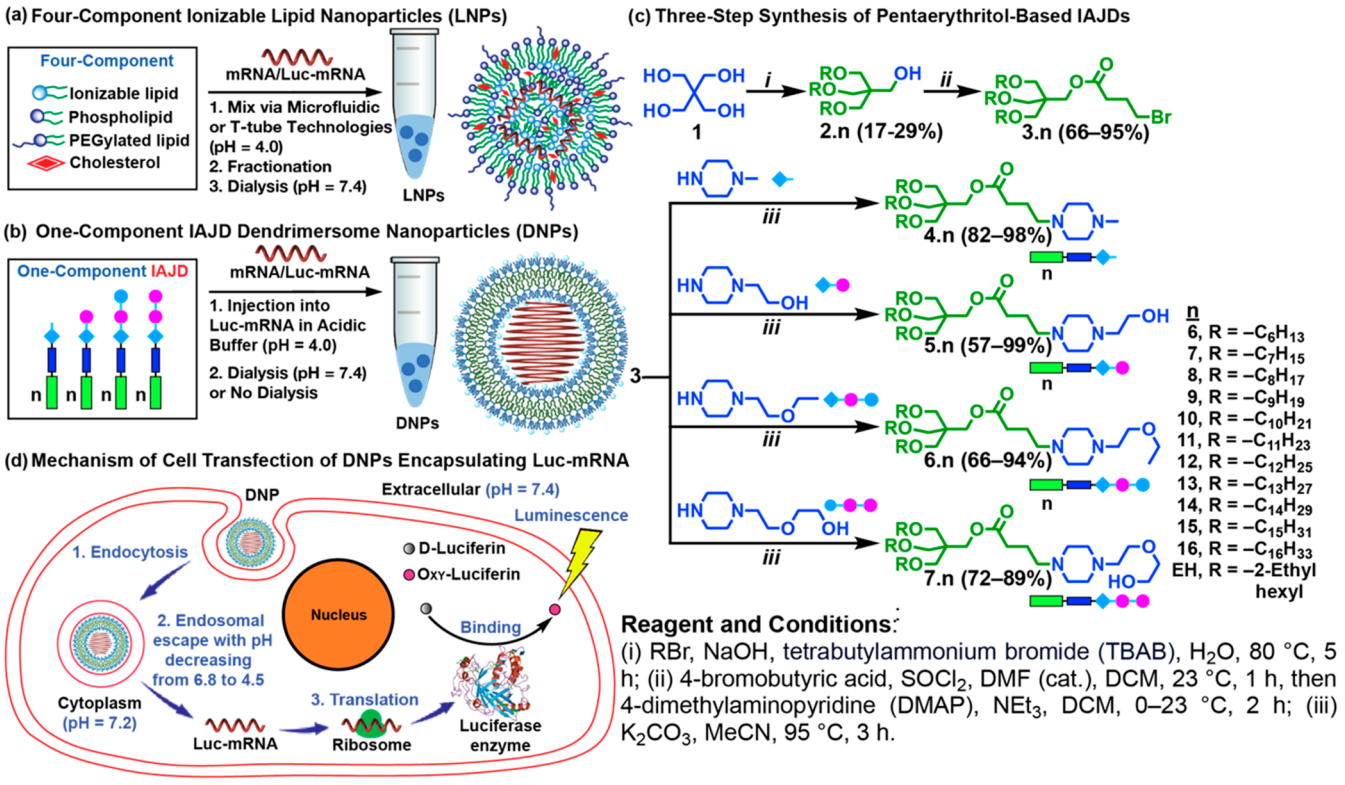

Figure 1. Concepts of four-component LNPs (a), one-component IAJD-based DNPs (b), three-step synthesis of PE-based IAJDs (c), and the mechanism of cell transfection of DNPs encapsulating Luc-mRNA (d).

coupled to one hydrophilic dendron containing IA), and simplified SS (sSS, obtained by removing the hydrophilic part of the hydrophilic dendron except for the IA) were first synthesized. Unexpectedly, sSS IAJD continued to self-assemble and coassemble into active DNPs. Phospholipids contain two *cis*-double bonds in their hydrophobic fragments. These *cis*-double bonds decrease the crystallization of their vesicle bilayer. To eliminate the oxidative instability of the bilayer, we constructed the hydrophobic domain with linear *n*-alkyl groups. However, these IAJDs crystallize at long alkyl lengths. Therefore, two dissimilar alkyl groups were incorporated into the hydrophobic part to perturb crystallization. While this composition was expected to decrease or eliminate crystallization, we could not predict that the resulting nonsymmetric sSS (nsSS) would exhibit up to 2 orders of magnitude higher delivery of mRNA. Rapid screening through IAJD libraries synthesized via modular-orthogonal methodologies and coassembly of IAJDs with mRNA into DNPs allowed discovery of molecular design principles for targeted delivery to the lung, liver, spleen, and lymph-nodes (LNs), for structures constructed from the plant phenolic 3,5-dihydroxybenzoic acid. Two sSS IAJDs constructed from PE alone,[5b] without organ analysis, did not provide encouraging results to pursue only PE as a branching point.[5a,b] The library constructed entirely from the PE branching point requires only three steps, fewer than any IAJD reported. The library of sSS PE-based IAJDs synthesized in this communication is outlined in Figure 1. *In vivo* experiments of these IAJDs coassembled with mRNA will demonstrate that the two sSS IAJDs reported previously[5b] were misleading because their mechanism of self-assembly is unlike that of IAJDs constructed from plant phenolic acids. Figure 1a illustrates the composition of the four-component LNPs coassembled with mRNA.[3c,g,i] Figure 1b shows the structures of the new IAJD library designed, synthesized (Figure 1c), and coassembled with mRNA. Figure 1d illustrates cell transfection. In the first step, PE (**1**) was alkylated under phase transfer catalyzed conditions[5a−d,8a−d] with the corresponding *n*-alkyl bromide (*n* = 6 to 16) or branched 2-ethylhexyl bromide (EH) in the presence of 50% NaOH at 80 °C for 5 h. After water addition, the mixture of tetraalkylated, trialkylated, and dialkylated PE together with the ether of the alkyl bromide formed was extracted with dichloromethane (DCM) and the trialkyl compounds **3** were separated by column chromatography (silica gel, hexane/ethyl acetate, 100/1 to 60/1) in about 20% yield. Compounds **2** were esterified with 4-bromobutyryl chloride or directly with 4-bromobutyric acid. 4-Bromobutyryl chloride was produced *in situ* from 4-bromobutyric acid and $SOCl_2$ in the presence of one drop of dry dimethylformamide (DMF) for 1 h followed by DCM and excess $SOCl_2$ distillation in a rotary evaporator. Esterification of **2** with 4-bromobutyryl chloride was performed at 0−23 °C for 2 h in dry DCM with NEt_3 base and 4-dimethylaminopyridine (DMAP) catalyst to generate the corresponding compounds **3** in about 85% yield after purification by column chromatography (silica gel, hexane/ethyl acetate, 100/1 to 60/1).

Compounds **3** were reacted with the four IAs, shown in Figure 1c, in MeCN in the presence of K_2CO_3 for 3 h[5a−d,8e] to provide IAJDs 4, 5, 6, and 7 in 80% to 90% yield (column chromatography, silica gel, DCM/MeOH, 50/1 to 20/1). The two IAs 6 and 7 were never used before in LNPs or IAJDs. The purity of all IAJDs determined by a combination of TLC, ^{1}H NMR, ^{13}C NMR, HPLC, and MALDI-TOFMS was higher than 99%. Figure S1 illustrates the chemical structures of all IAJDs synthesized as outlined in Figure 1c. IAJDs 285 and 101 (Figure S1) are solid, with the crystalline bilayer of their DNPs too stable to release the encapsulated mRNA.[7a] This is not unexpected

https://doi.org/10.1021/jacs.3c07337
J. Am. Chem. Soc. 2023, 145, 18760−18766

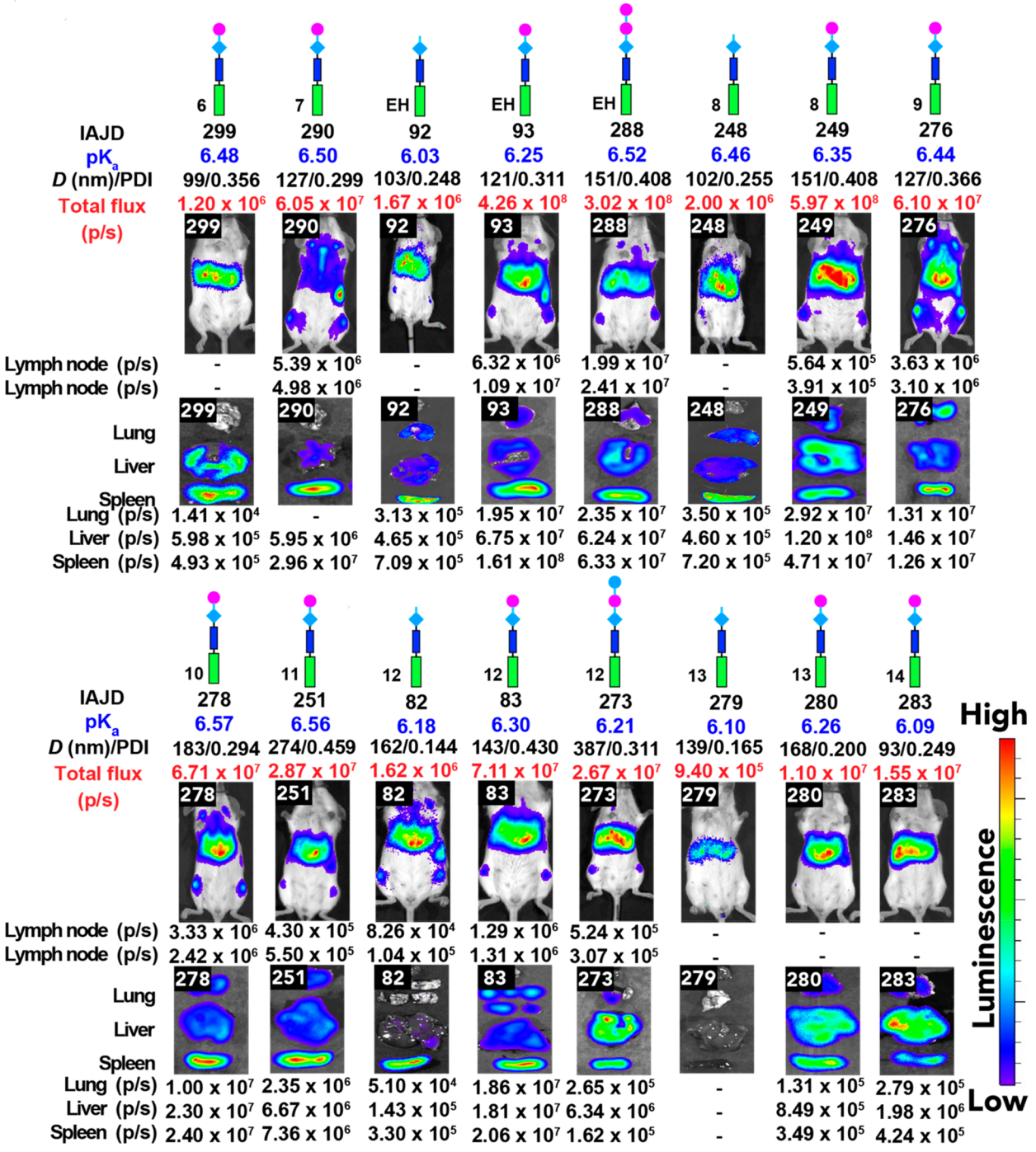

Figure 2. *In vivo* experiments of DNPs coassembled from PE-based IAJDs with Luc-mRNA.

since their alkyl groups contain 15 carbons for IAJD 285 and 16 for IAJD 101 and OH groups. All other IAJDs including 284 and 100 with 15 and 16 carbons but methyl piperazine IA are liquid at 23 °C. The pK_a values of all IAJDs in Figure S1 were determined and are listed after their schematic structure and number in Figure 2.

All IAJDs in Figure S1 were coassembled with Luc-mRNA by the ethanol injection method into acetate buffer containing Luc-mRNA (pH = 4.0).[5a−d] The dimensions and polydispersity of the resulting DNPs were determined by dynamic light scattering (DLS) and are summarized in Figure 2. Here we report screening experiments for which coassembly of IAJDs with mRNA and *in vivo* transfection experiments (Figure 2) were not optimized. DNP dimensions vary from 93 to 387 Å, and their polydispersities from 0.144 to 0.459. All methyl piperazine-based IAJDs show low *in vivo* luciferase activity with a total flux in the range of 10^6 p/s (see, for example, DSs derived from IAJDs 92, 248, 82, and 279) (Figures 2, 3).

IAJDs 289, 291, 292, 92, 287, 275, 277, 250, 274, 284, 285, 100, and 101 exhibit even lower transfection activity (not shown). Therefore, we incorrectly concluded that SS IAJDs 30 and 37[5a] and sSS 82[5b] were of no interest to employ the trialkyl-PE strategy as hydrophobic dendron. A single exception was provided by SS IAJD 31,[5a] which exhibited high transfection to lung, 1.4×10^8, but required an 18-step synthesis. However, the new sSS IAJDs 93, 288, and 249 exhibit a total flux of 4.26×10^8,

https://doi.org/10.1021/jacs.3c07337
J. Am. Chem. Soc. 2023, 145, 18760−18766

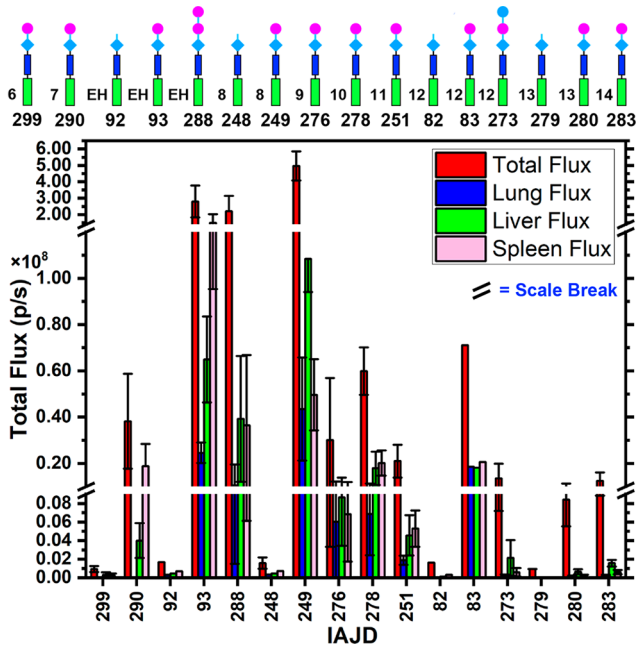

Figure 3. Comparison of total flux and spleen, liver, and lung flux of DNPs assembled from PE-based IAJDs demonstrating the structure–activity dependence.

3.02×10^8, and 5.97×10^8 p/s. *These values are equal to and even higher than the highest activities reported with IAJD-based DNPs.*[5a−d] The highest total activity detected for an IAJD was 4.05×10^8 for nsSS 178, containing a combination of 13 and 18 alkyl groups in its hydrophobic domain.[5c,d] IAJDs providing total flux activities higher than 10^8 p/s were discovered only for nsSS IAJDs.[5c,d] No sSS IAJDs containing identical alkyl group length in the hydrophobic part showed a higher total flux activity than 10^7.[5b−d] The total flux results reported here for IAJDs 93, 288, and 249 are remarkable considering that they are not optimized and require only a three-step synthesis. The highest total flux observed was for LNPs based on MC3 (1.7×10^9), which delivers to the liver. More interesting is the total flux activity per organ for these IAJDs. IAJD 93 delivers with an activity of 1.61×10^8 to the spleen and about 10^7 to LNs and higher than 10^7 to the liver and lung. LNPs based on MC3 deliver to the spleen with an activity of only 10^7.[5a] IAJD 249 delivered 1.20×10^8 activity to the liver. This liver activity is higher than the largest value obtained for an nsSS IAJD.[5c,d] Finally, IAJD 288 delivers with 6.33×10^7 and 6.24×10^7 to the spleen and liver and a lower 10^7 range activity to the lung and LN. This very high combination of equal delivery to the spleen, liver, and LNs *was never encountered before with any vector* and is best illustrated in Figure 3. All other DNPs based on IAJDs that do not contain methyl piperazine deliver equally with a total flux in the range of 10^7 to the spleen, liver, lung, and LNs (see IAJDs 276, 278, 251,83, 273, 280, 283). IAJD 290 delivers predominantly to the spleen, while 299 delivers equally to the spleen and liver. *This equally distributed delivery of mRNA has not been observed before with any viral or synthetic vectors* and *has an unknown mechanism but potential applications to cure diseases present in multiple organs*. The maximum total flux activity was observed for *n*-octyl in IAJD 249 and 2-EH in IAJD 93 and IAJD 288. Surprisingly, the transition from trinonyl IAJD 276 and trihexyl IAJD 299 to trioctyl IAJD 249, triEH IAJDs 288 and 93, and triheptyl IAJD 290 substituted PE (Figure 3) *induces the change from equally distributed delivery to targeted distributed delivery of mRNA*. Conversely, as the length of the *n*-alkyl of the IAJD increases, the total flux activity equally distributed to different organs decreases from the range of 10^8 and 10^7 for IAJD 93, 288, 248, 279, and 278 to a total flux per mouse of 10^7 for IAJD 83, 273, 280, and 283 with even lower total flux values per organ. *This is the opposite trend from the one observed with nsSS IAJDs that had the highest total flux activity for combinations of long alkyl groups.*[5d] *This reverse trend is determined by the different mechanism, stability, and number of steps of bilayer formation of these two DNPs* (Figure 4 and supplemental movies). *In the case of 3,5-dihydroxybenzoic acid-based DNPs the bilayer is assembled, most probably, by stepwise interdigitation of long alkyl groups and π−π stacking of benzyl parts, while in the case of PE-based IAJDs a similar bilayer width is generated by more efficient concerted end-to-end arrangement of short column-like alkyl group assembly* (Figure 4, supplemental movies). A preliminary estimate shows higher stability for IAJDs 249 vs 89 bilayers (Figure 4). In conclusion, PE-based IAJDs are mechanistically unrelated one-component delivery systems from the 3,5-dihydroxybenzoic acid-based IAJDs reported previously.[5a−d] They provide even higher total flux activity than nsSS IAJDs, although their structure belongs to the sSS IAJD systems.[5b−d] Most importantly, they are prepared in only three reaction steps. Depending on their alkyl group length, they facilitated *the discovery* of equal or targeted delivery of mRNA to a diversity of organs, with medical applications. Furthermore, one-component DNPs exhibit higher stability than the corresponding four-component LNPs, due to their symmetric achiral, rather than chiral architecture.[9] Four-component LNPs were also designed for targeted delivery[10a] and adjuvant activity.[10b] However, both required an increased number of LNP components from four to five.[10]

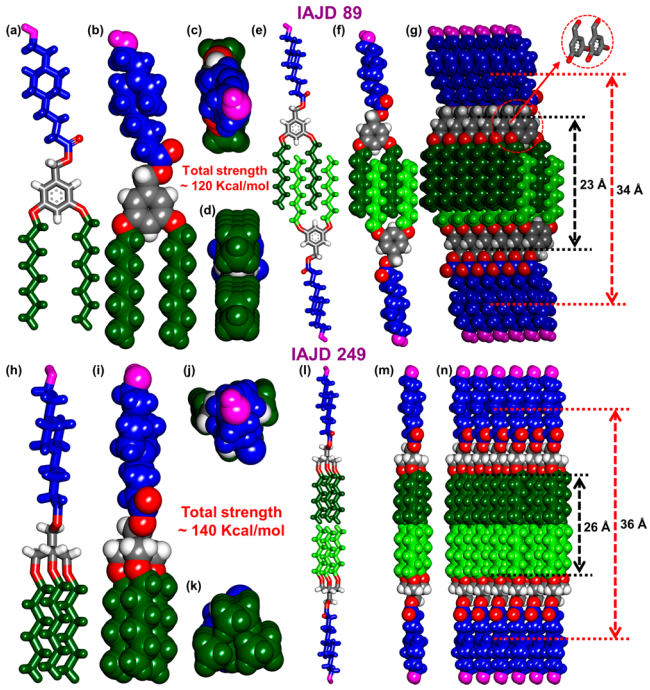

Figure 4. Structures of IAJD895b in stick-and-space-filled models in side views (a, b), top (c) and bottom views (c, d), interdigitated (e, f), and in membrane bilayer (g) and of IAJD249 side views (h, i), top and bottom views (j, k), end to end (l, m), and in membrane bilayer (n). Movies of bilayer self-assembly are in Supplemental Movies 1 and 2.

https://doi.org/10.1021/jacs.3c07337
J. Am. Chem. Soc. 2023, 145, 18760−18766

■ ASSOCIATED CONTENT

Supporting Information

The Supporting Information is available free of charge at https://pubs.acs.org/doi/10.1021/jacs.3c07337.

Supplemental Movie 1 (MP4)

Supplemental Movie 2 (MP4)

Experimental methods; complete experimental details for the synthesis and structural characterization of all 29 IAJDs with ^{1}H NMR, ^{13}C NMR, HPLC, and MALDI-TOFMS data; dimensions and polydispersities of their DNPs with mRNA and original DLS traces; all pK_a measurements and calculations; supplemental references (PDF)

■ AUTHOR INFORMATION

Corresponding Authors

Drew Weissman − *Department of Medicine, Perelman School of Medicine, University of Pennsylvania, Philadelphia, Pennsylvania 19104, United States;* orcid.org/0000-0002-1501-6510; Email: dreww@pennmedicine.upenn.edu

Virgil Percec − *Roy & Diana Vagelos Laboratories, Department of Chemistry, University of Pennsylvania, Philadelphia, Pennsylvania 19104-6323, United States;* orcid.org/0000-0001-5926-0489; Email: percec@sas.upenn.edu

Authors

Juncheng Lu − *Roy & Diana Vagelos Laboratories, Department of Chemistry, University of Pennsylvania, Philadelphia, Pennsylvania 19104-6323, United States*

Elena N. Atochina-Vasserman − *Department of Medicine, Perelman School of Medicine, University of Pennsylvania, Philadelphia, Pennsylvania 19104, United States;* orcid.org/0000-0001-7950-7004

Devendra S. Maurya − *Roy & Diana Vagelos Laboratories, Department of Chemistry, University of Pennsylvania, Philadelphia, Pennsylvania 19104-6323, United States;* orcid.org/0000-0002-4488-9927

Dipankar Sahoo − *Roy & Diana Vagelos Laboratories, Department of Chemistry, University of Pennsylvania, Philadelphia, Pennsylvania 19104-6323, United States; Department of Medicine, Perelman School of Medicine, University of Pennsylvania, Philadelphia, Pennsylvania 19104, United States*

Nathan Ona − *Department of Medicine, Perelman School of Medicine, University of Pennsylvania, Philadelphia, Pennsylvania 19104, United States*

Erin K. Reagan − *Department of Medicine, Perelman School of Medicine, University of Pennsylvania, Philadelphia, Pennsylvania 19104, United States;* orcid.org/0000-0003-3162-4636

Houping Ni − *Department of Medicine, Perelman School of Medicine, University of Pennsylvania, Philadelphia, Pennsylvania 19104, United States*

Complete contact information is available at: https://pubs.acs.org/10.1021/jacs.3c07337

Author Contributions

J.L. and E.N.A.-V. contributed equally to this work.

Notes

The authors declare no competing financial interest.

■ ACKNOWLEDGMENTS

This work was supported by National Science Foundation Grants DMR-2104554 and DMR-1720530, the P. Roy Vagelos Chair at the University of Pennsylvania, the Alexander von Humboldt Foundation (all to V.P.), and the Wellcome Leap R3 Program (to D.W. and V.P.). NMR Instrumentation (NEO400) was supported by the NSF Major Research Instrumentation Program (award NSF CHE-1827457) and Vagelos Institute for Energy Science and Technology.

■ REFERENCES

(1) (a) Whitehead, K. A.; Langer, R.; Anderson, D. G. Knocking down Barriers: Advances in SiRNA Delivery. *Nat. Rev. Drug Discovery*, **2009**, *8*, 129−138. (b) Cullis, P. R.; Hope, M. J. Lipid Nanoparticle Systems for Enabling Gene Therapies. *Mol. Ther*, **2017**, *25*, 1467−1475. (c) Buschmann, M. D.; Carrasco, M. J.; Alishetty, S.; Paige, M.; Alameh, M. G.; Weissman, D. Nanomaterial Delivery Systems for mRNA Vaccines. *Vaccines* **2021**, *9*, 65. (d) Wilson, J. M. Genetic Diseases, Immunology, Viruses, and Gene Therapy. *Hum. Gene Ther.* **2014**, *25*, 257−261. (e) Nguyen, J.; Szoka, F. C. Nucleic Acid Delivery: The Missing Pieces of the Puzzle? *Acc. Chem. Res.* **2012**, *45*, 1152−1162. (f) Lacroix, A.; Sleiman, H. F. DNA Nanostructures: Current Challenges and Opportunities for Cellular Delivery. *ACS Nano* **2021**, *15*, 3631−3645. (g) Billingsley, M. M.; Singh, N.; Ravikumar, P.; Zhang, R.; June, C. H.; Mitchell, M. J. Ionizable Lipid Nanoparticle-Mediated mRNA Delivery for Human CAR T Cell Engineering. *Nano Lett.* **2020**, *20*, 1578−1589. (h) Huang, X.; Kong, N.; Zhang, X.; Cao, Y.; Langer, R.; Tao, W. The Landscape of mRNA Nanomedicine. *Nat. Med.* **2022**, *28*, 2273−2287. (i) Yin, H.; Kanasty, R. L.; Eltoukhy, A. A.; Vegas, A. J.; Dorkin, J. R.; Anderson, D. G. Non-Viral Vectors for Gene-Based Therapy. *Nat. Rev. Genet.* **2014**, *15*, 541−555.

(2) (a) Luo, D.; Saltzman, W. M. Synthetic DNA Delivery Systems. *Nat. Biotechnol.* **2000**, *18*, 33−37. (b) Wickham, T. J. Ligand-Directed Targeting of Genes to the Site of Disease. *Nat. Med.* **2003**, *9*, 135−139. (c) Hajj, K. A.; Whitehead, K. A. Tools for Translation: Non-Viral Materials for Therapeutic mRNA Delivery. *Nat. Rev. Mater.* **2017**, *2*, 1−17. (d) Ramamoorth, M.; Narvekar, A. Non Viral Vectors in Gene Therapy- an Overview. *J. Clin. Diagn. Res.* **2015**, *9*, GE01−06. (e) Baum, C.; Kustikova, O.; Modlich, U.; Li, Z.; Fehse, B. Mutagenesis and Oncogenesis by Chromosomal Insertion of Gene Transfer Vectors. *Hum. Gene. Ther.* **2006**, *17*, 253−263. (f) Bessis, N.; GarciaCozar, F. J.; Boissier, M.-C. Immune Responses to Gene Therapy Vectors: Influence on Vector Function and Effector Mechanisms. *Gene Ther.* **2004**, *11*, S10−S17. (g) Bouard, D.; Alazard-Dany, D.; Cosset, F.-L. Viral Vectors: From Virology to Transgene Expression. *Br. J. Pharmacol.* **2009**, *157*, 153−165.

(3) (a) Chen, D.; Love, K. T.; Chen, Y.; Eltoukhy, A. A.; Kastrup, C.; Sahay, G.; Jeon, A.; Dong, Y.; Whitehead, K. A.; Anderson, D. G. Rapid Discovery of Potent Sirna-Containing Lipid Nanoparticles Enabled by Controlled Microfluidic Formulation. *J. Am. Chem. Soc.* **2012**, *134*, 6948−6951. (b) Zhigaltsev, I. V.; Belliveau, N.; Hafez, I.; Leung, A. K.; Huft, J.; Hansen, C.; Cullis, P. R. Bottom-up Design and Synthesis of Limit Size Lipid Nanoparticle Systems with Aqueous and Triglyceride Cores Using Millisecond Microfluidic Mixing. *Langmuir* **2012**, *28*, 3633−3640. (c) Leung, A. K.; Hafez, I. M.; Baoukina, S.; Belliveau, N. M.; Zhigaltsev, I. V.; Afshinmanesh, E.; Tieleman, D. P.; Hansen, C. L.; Hope, M. J.; Cullis, P. R. Lipid Nanoparticles Containing Sirna Synthesized by Microfluidic Mixing Exhibit an Electron-Dense Nanostructured Core. *J. Phys. Chem. C* **2012**, *116*, 18440−18450. (d) Leung, A. K.; Tam, Y. Y.; Chen, S.; Hafez, I. M.; Cullis, P. R. Microfluidic Mixing: A General Method for Encapsulating Macromolecules in Lipid Nanoparticle Systems. *J. Phys. Chem. B* **2015**, *119*, 8698−8706. (e) Pardi, N.; Hogan, M. J.; Porter, F. W.; Weissman, D. mRNA Vaccines — a New Era in Vaccinology. *Nat. Rev. Drug Discovery* **2018**, *17*, 261−279. (f) Jayaraman, M.; Ansell, S. M.; Mui, B. L.; Tam, Y. K.; Chen, J.; Du, X.; Butler, D.; Eltepu, L.; Matsuda, S.; Narayanannair, J. K.; Rajeev, K. G.; Hafez, I. M.; Akinc, A.; Maier, M.

A.; Tracy, M. A.; Cullis, P. R.; Madden, T. D.; Manoharan, M.; Hope, M. J. Maximizing the Potency of siRNA Lipid Nanoparticles for Hepatic Gene Silencing In Vivo. *Angew. Chem., Int. Ed.* **2012**, *51*, 8529−8533. (g) Kulkarni, J. A.; Witzigmann, D.; Chen, S.; Cullis, P. R.; van der Meel, R. Lipid Nanoparticle Technology for Clinical Translation of siRNA Therapeutics. *Acc. Chem. Res.* **2019**, *52*, 2435−2444. (h) Ramezanpour, M.; Schmidt, M. L.; Bodnariuc, I.; Kulkarni, J. A.; Leung, S. S. W.; Cullis, P. R.; Thewalt, J. L.; Tieleman, D. P. Ionizable Amino Lipid Interactions with POPC: Implications for Lipid Nanoparticle Function. *Nanoscale* **2019**, *11*, 14141−14146. (i) Kulkarni, J. A.; Darjuan, M. M.; Mercer, J. E.; Chen, S.; van der Meel, R.; Thewalt, J. L.; Tam, Y. Y. C.; Cullis, P. R. On the Formation and Morphology of Lipid Nanoparticles Containing Ionizable Cationic Lipids and siRNA. *ACS Nano* **2018**, *12*, 4787−4795. (j) Hatakeyama, H.; Akita, H.; Harashima, H. A Multifunctional Envelope Type Nano Device (MEND) for Gene Delivery to Tumours Based on the EPR Effect: A Strategy for Overcoming the PEG Dilemma. *Adv. Drug Delivery Rev.* **2011**, *63*, 152−160. (k) Sato, Y.; Hatakeyama, H.; Sakurai, Y.; Hyodo, M.; Akita, H.; Harashima, H. A pH-Sensitive Cationic Lipid Facilitates the Delivery of Liposomal siRNA and Gene Silencing Activity in Vitro and in Vivo. *J. Controlled Release* **2012**, *163*, 267−276. (l) Choi, J. S.; MacKay, J. A.; Szoka, F. C. Low-pH-Sensitive PEG-Stabilized Plasmid−Lipid Nanoparticles: Preparation and Characterization. *Bioconjugate Chem.* **2003**, *14*, 420−429. (m) Pelegri-O'Day, E. M.; Lin, E.-W.; Maynard, H. D. Therapeutic Protein−Polymer Conjugates: Advancing Beyond PEGylation. *J. Am. Chem. Soc.* **2014**, *136*, 14323−14332. (n) Whitfield, C. J.; Zhang, M.; Winterwerber, P.; Wu, Y.; Ng, D. Y. W.; Weil, T. Functional DNA−Polymer Conjugates. *Chem. Rev.* **2021**, *121*, 11030.

(4) (a) Kukowska-Latallo, J. F.; Bielinska, A. U.; Johnson, J.; Spindler, R.; Tomalia, D. A.; Baker, J. R. Efficient Transfer of Genetic Material into Mammalian Cells Using Starburst Polyamidoamine Dendrimers. *Proc. Natl. Acad. Sci. U.S.A.* **1996**, *93*, 4897−4902. (b) Zhou, J.; Wu, J.; Hafdi, N.; Behr, J.-P.; Erbacher, P.; Peng, L. PAMAM Dendrimers for Efficient SiRNA Delivery and Potent Gene Silencing. *Chem. Commun.* **2006**, No. 22, 2362. (c) Posadas, I.; Guerra, F.; Cena, V. Nonviral Vectors for the Delivery of Small Interfering RNAs to the CNS. *Nanomed* **2010**, *5*, 1219−1236. (d) Rodrigo, A. C.; Rivilla, I.; Perez-Martinez, F. C.; Monteagudo, S.; Ocana, V.; Guerra, J.; Garcia-Martinez, J. C.; Merino, S.; Sanchez-Verdu, P.; Cena, V.; Rodríguez-López, J. Efficient, Non-Toxic Hybrid PPV-PAMAM Dendrimer as a Gene Carrier for Neuronal Cells. *Biomacromolecules* **2011**, *12*, 1205−1213. (e) Majoral, J.-P.; Caminade, A. M. Dendrimers Containing Heteroatoms (Si, P, B, Ge, or Bi). *Chem. Rev.* **1999**, *99*, 845−880. (f) Janiszewska, J.; Posadas, I.; Jativa, P.; Bugaj-Zarebska, M.; Urbanczyk-Lipkowska, Z.; Cena, V. Second Generation Amphiphilic Poly-Lysine Dendrons Inhibit Glioblastoma Cell Proliferation without Toxicity for Neurons or Astrocytes. *PLoS One* **2016**, *11*, No. e0165704. (g) Haensler, J.; Szoka, F. C., Jr Polyamidoamine Cascade Polymers Mediate Efficient Transfection of Cells in Culture. *Bioconjugate Chem.* **1993**, *4*, 372−379. (h) Loup, C.; Zanta, M.-A.; Caminade, A.-M.; Majoral, J.-P.; Meunier, B. Preparation of Water-Soluble Cationic Phosphorus-Containing Dendrimers as DNA Transfecting Agents. *Chem.—Eur. J.* **1999**, *5*, 3644−3650. (i) Pedziwiatr, E.; Chonco, L.; Shcharbin, D.; de Jesus, E.; Bermejo, J. F.; Ortega, P.; de la Mata, F. J.; Flores, J. C.; Gomez, R.; Klajnert, B.; Munoz-Fernandez, M. A.; Bryszewska, M. Carbosilane Dendrimers as Drug Carriers. *Eur. J. Clin. Invest.* **2007**, *37*, 79−79. (j) Zinselmeyer, B. H.; Mackay, S. P.; Schatzlein, A. G.; Uchegbu, I. F. The Lower-Generation Polypropylenimine Dendrimers Are Effective Gene-Transfer Agents. *Pharm. Res.* **2002**, *19*, 960−967.

(5) (a) Zhang, D.; Atochina-Vasserman, E. N.; Maurya, D. S.; Huang, N.; Xiao, Q.; Ona, N.; Liu, M.; Shahnawaz, H.; Ni, H.; Kim, K.; Billingsley, M. M.; Pochan, D. J.; Mitchell, M. J.; Weissman, D.; Percec, V. One-Component Multifunctional Sequence-Defined Ionizable Amphiphilic Janus Dendrimer Delivery Systems for mRNA. *J. Am. Chem. Soc.* **2021**, *143*, 12315−12327. (b) Zhang, D.; Atochina-Vasserman, E. N.; Maurya, D. S.; Liu, M.; Xiao, Q.; Lu, J.; Lauri, G.; Ona, N.; Reagan, E. K.; Ni, H.; Weissman, D.; Percec, V. Targeted Delivery of MRNA with One-Component Ionizable Amphiphilic Janus Dendrimers. *J. Am. Chem. Soc.* **2021**, *143*, 17975−17982. (c) Zhang, D.; Atochina-Vasserman, E. N.; Lu, J.; Maurya, D. S.; Xiao, Q.; Liu, M.; Adamson, J.; Ona, N.; Reagan, E. K.; Ni, H.; Weissman, D.; Percec, V. The Unexpected Importance of the Primary Structure of the Hydrophobic Part of One-Component Ionizable Amphiphilic Janus Dendrimers in Targeted MRNA Delivery Activity. *J. Am. Chem. Soc.* **2022**, *144*, 4746−4753. (d) Lu, J.; Atochina-Vasserman, E. N.; Maurya, D. S.; Shalihin, M. I.; Zhang, D.; Chenna, S. S.; Adamson, J.; Liu, M.; Shah, H. U. R.; Shah, H.; Xiao, Q.; Queeley, B.; Ona, N. A.; Reagan, E. K.; Ni, H.; Sahoo, D.; Peterca, M.; Weissman, D.; Percec, V. Screening Libraries to Discover Molecular Design Principles for the Targeted Delivery of MRNA with One-Component Ionizable Amphiphilic Janus Dendrimers Derived from Plant Phenolic Acids. *Pharmaceutics* **2023**, *15*, 1572.

(6) (a) Percec, V.; Wilson, D. A.; Leowanawat, P.; Wilson, C. J.; Hughes, A. D.; Kaucher, M. S.; Hammer, D. A.; Levine, D. H.; Kim, A. J.; Bates, F. S.; Davis, K. P.; Lodge, T. P.; Klein, M. L.; DeVane, R. H.; Aqad, E.; Rosen, B. M.; Argintaru, A. O.; Sienkowska, M. J.; Rissanen, K.; Nummelin, S. Self-Assembly of Janus Dendrimers into Uniform Dendrimersomes and Other Complex Architectures. *Science* **2010**, *328*, 1009−1014. (b) Sherman, S. E.; Xiao, Q.; Percec, V. Mimicking Complex Biological Membranes and Their Programmable Glycan Ligands with Dendrimersomes and Glycodendrimersomes. *Chem. Rev.* **2017**, *117*, 6538−6631. (c) Peterca, M.; Percec, V.; Leowanawat, P.; Bertin, A. Predicting the Size and Properties of Dendrimersomes from the Lamellar Structure of Their Amphiphilic Janus Dendrimers. *J. Am. Chem. Soc.* **2011**, *133*, 20507−20520. (d) Zhang, S.; Sun, H.-J.; Hughes, A. D.; Draghici, B.; Lejnieks, J.; Leowanawat, P.; Bertin, A.; Otero De Leon, L.; Kulikov, O. V.; Chen, Y.; Pochan, D. J.; Heiney, P. A.; Percec, V. Single−Single" Amphiphilic Janus Dendrimers Self-Assemble into Uniform Dendrimersomes with Predictable Size. *ACS Nano* **2014**, *8*, 1554−1565. (e) Zhang, S.; Sun, H.-J.; Hughes, A. D.; Moussodia, R.-O.; Bertin, A.; Chen, Y.; Pochan, D. J.; Heiney, P. A.; Klein, M. L.; Percec, V. Self-Assembly of Amphiphilic Janus Dendrimers into Uniform Onion-Like Dendrimersomes with Predictable Size and Number of Bilayers. *Proc. Natl. Acad. Sci. U. S. A.* **2014**, *111*, 9058−9063. (f) Xiao, Q.; Yadavalli, S. S.; Zhang, S.; Sherman, S. E.; Fiorin, E.; Silva, L. d.; Wilson, D. A.; Hammer, D. A.; André, S.; Gabius, H.-J.; Klein, M. L.; Goulian, M.; Percec, V. Bioactive Cell-Like Hybrids Coassembled from (Glyco)Dendrimersomes with Bacterial Membranes. *Proc. Natl. Acad. Sci. U. S. A.* **2016**, *113*, No. E1134-E1141. (g) Yadavalli, S. S.; Xiao, Q.; Sherman, S. E.; Hasley, W. D.; Klein, M. L.; Goulian, M.; Percec, V. Bioactive Cell-Like Hybrids from Dendrimersomes with a Human Cell Membrane and Its Components. *Proc. Natl. Acad. Sci. U. S. A.* **2019**, *116*, 744−752. (h) Xiao, Q.; Sherman, S. E.; Wilner, S. E.; Zhou, X.; Dazen, C.; Baumgart, T.; Reed, E. H.; Hammer, D. A.; Shinoda, W.; Klein, M. L.; Percec, V. Janus Dendrimersomes Coassembled from Fluorinated, Hydrogenated, and Hybrid Janus Dendrimers as Models for Cell Fusion and Fission. *Proc. Natl. Acad. Sci. U. S. A.* **2017**, *114*, No. E7045-E7053. (i) Torre, P.; Xiao, Q.; Buzzacchera, I.; Sherman, S. E.; Rahimi, K.; Kostina, N. Y.; Rodriguez-Emmenegger, C.; Möller, M.; Wilson, C. J.; Klein, M. L.; Good, M. C.; Percec, V. Encapsulation of Hydrophobic Components in Dendrimersomes and Decoration of Their Surface with Proteins and Nucleic Acids. *Proc. Natl. Acad. Sci. U. S. A.* **2019**, *116*, 15378−15385. (j) Li, S.; Xia, B.; Javed, B.; Hasley, W. D.; Melendez-Davila, A.; Liu, M.; Kerzner, M.; Agarwal, S.; Xiao, Q.; Torre, P.; Bermudez, J. G.; Rahimi, K.; Kostina, N. Yu.; Möller, M.; Rodriguez-Emmenegger, C.; Klein, M. L.; Percec, V.; Good, M. C. Direct Visualization of Vesicle Disassembly and Reassembly Using Photocleavable Dendrimers Elucidates Cargo Release Mechanisms. *ACS Nano* **2020**, *14*, 7398−7411. (k) Kostina, N. Y.; Wagner, A. M.; Haraszti, T.; Rahimi, K.; Xiao, Q.; Klein, M. L.; Percec, V.; Rodriguez-Emmenegger, C. Unraveling Topology-Induced Shape Transformations in Dendrimersomes. *Soft Matter* **2021**, *17*, 254−267. (l) Kostina, N. Yu.; Rahimi, K.; Xiao, Q.; Haraszti, T.; Dedisch, S.; Spatz, J. P.; Schwaneberg, U.; Klein, M. L.; Percec, V.; Möller, M.; Rodriguez-Emmenegger, C. Membrane-Mimetic Dendrimersomes Engulf Living Bacteria via Endocytosis. *Nano Lett.* **2019**, *19*,

https://doi.org/10.1021/jacs.3c07337
J. Am. Chem. Soc. 2023, 145, 18760−18766

5732−5738. (m) Buzzacchera, I.; Xiao, Q.; Han, H.; Rahimi, K.; Li, S.; Kostina, N. Y.; Toebes, B. J.; Wilner, S. E.; Möller, M.; Rodriguez-Emmenegger, C.; Baumgart, T.; Wilson, D. A.; Wilson, C. J.; Klein, M. L.; Percec, V. Screening Libraries of Amphiphilic Janus Dendrimers based on Natural Phenolic Acids to Discover Monodisperse Unilamellar Dendrimersomes. *Biomacromolecules* **2019**, *20*, 712−727. (n) Rosen, B. M.; Wilson, C. J.; Wilson, D. A.; Peterca, M.; Imam, M. R.; Percec, V. Dendron-Mediated Self-Assembly, Disassembly, and Self-Organization of Complex Systems. *Chem. Rev.* **2009**, *109*, 6275−6540. (o) Sun, H.-J.; Zhang, S.; Percec, V. From Structure to Function via Complex Supramolecular Dendrimer Systems. *Chem. Soc. Rev.* **2015**, *44*, 3900−3923. (p) Kopitz, J.; Xiao, Q.; Ludwig, A.-K.; Romero, A.; Michalak, M.; Sherman, S. E.; Zhou, X.; Dazen, C.; Vértesy, S.; Kaltner, H.; Klein, M. L.; Gabius, H.-J.; Percec, V. Reaction of a Programmable Glycan Presentation of Glycodendrimersomes and Cells with Engineered Human Lectins To Show the Sugar Functionality of the Cell Surface. *Angew. Chem., Int. Ed.* **2017**, *56*, 14677−14681. (q) Ludwig, A.-K.; Michalak, M.; Xiao, Q.; Gilles, U.; Medrano, F. J.; Ma, H.; FitzGerald, F. G.; Hasley, W. D.; Melendez-Davila, A.; Liu, M.; Rahimi, K.; Kostina, N. Y.; Rodriguez-Emmenegger, C.; Möller, M.; Lindner, I.; Kaltner, H.; Cudic, M.; Reusch, D.; Kopitz, J.; Romero, A.; Oscarson, S.; Klein, M. L.; Gabius, H.-J.; Percec, V. Design−Functionality Relationships for Adhesion/Growth-Regulatory Galectins. *Proc. Natl. Acad. Sci. U. S. A.* **2019**, *11*, 2837−2842. (r) Percec, V.; Xiao, Q. Helical Self-Organizations and Emerging Functions in Architectures, Biological and Synthetic Macromolecules. *BCSJ.* **2021**, *94*, 900−928. (s) Xiao, Q.; Ludwig, A.-K.; Romanò, C.; Buzzacchera, I.; Sherman, S. E.; Vetro, M.; Vértesy, S.; Kaltner, H.; Reed, E. H.; Möller, M.; Wilson, C. J.; Hammer, D. A.; Oscarson, S.; Klein, M. L.; Gabius, H.-J.; Percec, V. Exploring Functional Pairing between Surface Glycoconjugates and Human Galectins Using Programmable Glycodendrimersomes. *Proc. Natl. Acad. Sci. U. S. A.* **2018**, *115*, No. E2509-E2518. (t) Xiao, Q.; Rubien, J. D.; Wang, Z.; Reed, E. H.; Hammer, D. A.; Sahoo, D.; Heiney, P. A.; Yadavalli, S. S.; Goulian, M.; Wilner, S. E.; Baumgart, T.; Vinogradov, S. A.; Klein, M. L.; Percec, V. Self-Sorting and Coassembly of Fluorinated, Hydrogenated, and Hybrid Janus Dendrimers into Dendrimersomes. *J. Am. Chem. Soc.* **2016**, *138*, 12655−12663. (v) Zhang, S.; Moussodia, R.-O.; Sun, H.-J.; Leowanawat, P.; Muncan, A.; Nusbaum, C. D.; Chelling, K. M.; Heiney, P. A.; Klein, M. L.; André, S.; Roy, R.; Gabius, H.-J.; Percec, V. Mimicking Biological Membranes with Programmable Glycan Ligands Self-Assembled from Amphiphilic Janus Glycodendrimers. *Angew. Chem., Int. Ed.* **2014**, *53*, 10899−10903. (x) Zhang, S.; Moussodia, R.-O.; Murzeau, C.; Sun, H.-J.; Klein, M. L.; Vértesy, S.; André, S.; Roy, R.; Gabius, H.-J.; Percec, V. Dissecting Molecular Aspects of Cell Interactions Using Glycodendrimersomes with Programmable Glycan Presentation and Engineered Human Lectins. *Angew. Chem., Int. Ed.* **2015**, *54*, 4036−4040. (y) Zhang, S.; Moussodia, R.-O.; Vértesy, S.; André, S.; Klein, M. L.; Gabius, H.-J.; Percec, V. Unraveling Functional Significance of Natural Variations of a Human Galectin by Glycodendrimersomes with Programmable Glycan Surface. *Proc. Natl. Acad. Sci. U. S. A.* **2015**, *112*, 5585−5590.

(7) (a) Percec, V.; Leowanawat, P.; Sun, H.-J.; Kulikov, O.; Nusbaum, C. D.; Tran, T. M.; Bertin, A.; Wilson, D. A.; Peterca, M.; Zhang, S.; Kamat, N. P.; Vargo, K.; Moock, D.; Johnston, E. D.; Hammer, D. A.; Pochan, D. J.; Chen, Y.; Chabre, Y. M.; Shiao, T. C.; Bergeron-Brlek, M.; Andre, S.; Roy, R.; Gabius, H.-J.; Heiney, P. A. Modular Synthesis of Amphiphilic Janus Glycodendrimers and Their Self-Assembly into Glycodendrimersomes and Other Complex Architectures with Bioactivity to Biomedically Relevant Lectins. *J. Am. Chem. Soc.* **2013**, *135*, 9055−9077. (b) Zhang, S.; Xiao, Q.; Sherman, S. E.; Muncan, A.; Ramos Vicente, A. D. M.; Wang, Z.; Hammer, D. A.; Williams, D.; Chen, Y.; Pochan, D. J.; Vértesy, S.; André, S.; Klein, M. L.; Gabius, H.-J.; Percec, V. Glycodendrimersomes from Sequence-Defined Janus Glycodendrimers Reveal High Activity and Sensor Capacity for the Agglutination by Natural Variants of Human Lectins. *J. Am. Chem. Soc.* **2015**, *137*, 13334−13344. (c) Xiao, Q.; Zhang, S.; Wang, Z.; Sherman, S. E.; Moussodia, R.-O.; Peterca, M.; Muncan, A.; Williams, D. R.; Hammer, D. A.; Vértesy, S.; André, S.; Gabius, H.-J.; Klein, M. L.; Percec, V. Onion-like Glycodendrimersomes from Sequence-Defined Janus Glycodendrimers and Influence of Architecture on Reactivity to a Lectin. *Proc. Natl. Acad. Sci. U. S. A.* **2016**, *113*, 1162−1167. (d) Rodriguez-Emmenegger, C.; Xiao, Q.; Kostina, N. Y.; Sherman, S. E.; Rahimi, K.; Partridge, B. E.; Li, S.; Sahoo, D.; Perez, A. M. R.; Buzzacchera, I.; Han, H.; Kerzner, M.; Malhotra, I.; Möller, M.; Wilson, C. J.; Good, M. C.; Goulian, M.; Baumgart, T.; Klein, M. L.; Virgil Percec, V. Encoding Biological Recognition in a Bicomponent Cell-Membrane Mimic. *Proc. Natl. Acad. Sci. U. S. A.* **2019**, *116*, 5376−5382. (e) Xiao, Q.; Delbianco, M.; Sherman, S. E.; Perez, A. M. R.; Bharate, P.; Pardo-Vargas, A.; Rodriguez-Emmenegger, C.; Kostina, N. Y.; Rahimi, K.; Söder, D.; Möller, M.; Klein, M. L.; Seeberger, P. H.; Percec, V. Nanovesicles Displaying Functional Linear and Branched Oligomannose Self-Assembled from Sequence-Defined Janus Glycodendrimers. *Proc. Natl. Acad. Sci. U. S. A.* **2020**, *117*, 11931−11939. (f) Kostina, N. Y.; Söder, D.; Haraszti, T.; Xiao, Q.; Rahimi, K.; Partridge, B. E.; Klein, M. L.; Percec, V.; Rodriguez-Emmenegger, C. Enhanced Concanavalin A Binding to Preorganized Mannose Nanoarrays in Glycodendrimersomes Revealed Multivalent Interactions. *Angew. Chem., Int. Ed.* **2021**, *60*, 8352−8360.

(8) (a) Nouguier, R. M.; Mchicj, M. Alkylation of Pentaerythritol and Trimethylolpropane, Two Very Hydrophilic Polyols, by Phase-Transfer Catalysis. *J. Org. Chem.* **1985**, *50*, 3296−3298. (b) Nouguier, R. M.; Mchicj, M. Alkylation of Pentaerythritol by Phase-Transfer Catalysis. 2. Crucial Effect of Aqueous Sodium Hydroxide Solution. *Tetrahedron* **1988**, *44*, 2477−2481. (c) Nouguier, R. M.; Mchicj, M. Alkylation of Pentaerythritol by Phase-Transfer Catalysis. 3. Influence of the Tetrahedral Structure of Pentaerythritol on the Rate and Selectivity of the Phase-Transfer-Catalyzed Reaction. *J. Org. Chem.* **1987**, *52*, 2995−2997. (d) Dumoulin, F.; Lafont, D.; Huynh, T.-L.; Boullanger, P.; Mackenzie, G.; West, J. J.; Goodby, J. W. Synthesis and Liquid Crystalline Properties of Mono-, Di and Tri-O-alkyl Pentaerythritol Derivatives Bearing Tri-, Di- or Monogalactosyl Heads: The Effects of Curvature of Molecular Packing on Mesophase Formation. *Chem.—Eur. J.* **2007**, *13*, 5585−5600. (e) May, J. P.; Undzys, E.; Roy, A.; Li, S.-D. Synthesis of a Gemcitabine Prodrug for Remote Loading into Liposomes and Improved Therapeutic Effect. *Bioconjugate Chem.* **2016**, *27*, 226−237.

(9) Zhang, D.; Xiao, Q. W.; Rahimzadeh, M.; Liu, M.; Rodriguez-Emmenegger, C.; Miyazaki, Y.; Shinoda, W.; Percec, V. Self-Assembly of Glycerol-Amphiphilic Dendrimers Amplifies and Indicates Principles for the Selection of Stereochemistry by Biological Membranes. *J. Am. Chem. Soc.* **2023**, *145*, 4311−4323.

(10) (a) Cheng, Q.; Wei, T.; Fabiak, L.; Johnson, L. T.; Dilliard, S. A.; Siegwart, D. J. Selective Organ Targeting (SORT) Nanoparticles for Tissue-Specific mRNA Delivery and CRISPR-Cas Gene Editing. *Nat. Nanotechnol.* **2020**, *15*, 313−320. (b) Han, X.; Alameh, M.-G.; Butowska, K.; Knox, J. J.; Lundgreen, K.; Ghattas, M.; Gong, N.; Xue, L.; Xu, Y.; Lavertu, M.; Bates, P.; Xu, J.; Nie, G.; Zhong, Y.; Weissman, D.; Mitchell, M. J. Adjuvant Lipidoid-Substituted Lipid Nanoparticles Augment the Immunogenicity of SARS-CoV-2 MRNA Vaccines. *Nat. Nanotechnol.* **2023**, DOI: 10.1038/s41565-023-01404-4.

https://doi.org/10.1021/jacs.3c07337
J. Am. Chem. Soc. 2023, 145, 18760−18766